Conversion of Anisole Catalyzed by Platinum Supported on Alumina: The Reaction Network

ARTICLE *in* ENERGY & FUELS · AUGUST 2011

Impact Factor: 2.79 · DOI: 10.1021/ef2010699

energy&fuels

ARTICLE

pubs.acs.org/EF

Conversion of Anisole Catalyzed by Platinum Supported on Alumina: The Reaction Network

Ron C. Runnebaum,[†] Rodrigo J. Lobo-Lapidus,[†,§] Tarit Nimmanwudipong,[†] David E. Block,[†,‡] and Bruce C. Gates*[,†]

[†]Department of Chemical Engineering and Materials Science, University of California, One Shields Avenue, Davis, California 95616, United States

[‡]Department of Viticulture and Enology, University of California, One Shields Avenue, Davis, California 95616, United States

Supporting Information

ABSTRACT: The conversion of anisole (a compound representative of bio-oils) in the presence of H_2 was investigated with a flow reactor operated at a temperature of 573 K and a pressure of 140 kPa with a platinum on alumina catalyst. Analysis by gas chromatography−mass spectrometry led to the identification of more than 40 reaction products, the most abundant being phenol, 2-methylphenol, benzene, and 2,6-dimethylphenol. The kinetically significant reaction classes were transalkylation, hydrodeoxygenation, and hydrogenation. Selectivity-conversion data were used to determine an approximate quantitative reaction network accounting for phenol, 2-methylphenol, 2-methylanisole, and 4-methylphenol as primary products. Pseudo-first-order rate constants for the formation of these products are 12, 2.8, 0.14, and 0.039 L/(g of catalyst × h), respectively. A more complete qualitative network was inferred on the basis of the observed products and the assumption that the reaction classes leading to the most abundant primary products were responsible for the minor and trace products. The removal of oxygen was evidenced by the production of benzene.

INTRODUCTION

Catalytic conversion of feedstocks formed by pyrolysis of cellulosic and lignin-rich biomass is an attractive option for the production of renewable liquid transportation fuels.[1−3] Although conversion data characterizing complex bio-oil feedstocks have been reported,[4−23] there is a lack of fundamental understanding of the classes of reactions involved. Sharma et al.[6−10] and Vitolo et al.[11] investigated the catalytic conversion of various bio-oils, with catalysts such as the zeolite HZSM-5. Adjaye et al.[12−14] focused on the conversion of fast pyrolysis bio-oils catalyzed by zeolites and silica−aluminas. A few researchers have investigated the catalytic hydrotreatment of bio-oils,[15−23] demonstrating significant removal of oxygen. The complexity of the feedstocks, however, limits the usefulness of these data for predicting the conversions of other feedstocks. In these investigations, the individual products found in the conversion of bio-oils have sometimes been grouped into classes (lumps), and approximate reaction networks showing conversion to the lumps have been reported.

The conversion of individual, prototypical bio-oil compounds has also been investigated by a number of researchers. The catalytic reaction networks presented by these researchers, which were determined from conversions measured in the absence of H_2, are limited either to primary products (or occasionally primary and secondary products) or to products that have been lumped into classes of similar compounds (e.g., phenol, alkylphenol, and alkylated ether lumps).[24−35]

Investigations of the reactions of individual compounds have been of value in advancing the understanding of petroleum and coal-liquid hydroprocessing reactions,[36] and they offer the prospect of having similar value for biomass conversion. Because today's instruments allow analysis of products in much more detail than was reported in early work defining the reactions of petroleum and coal refining, it is possible to determine reaction networks that are much more detailed than those reported in these early investigations. Our goal was to determine such a detailed reaction network for a compound representative of lignin-derived bio-oils and an important functional group characterizing compounds in them; consequently, we chose a compound, anisole, that is aromatic and incorporates an ether linkage.

The catalytic hydrotreating of anisole was investigated by Bredenberg et al.[37] and by Hurff and Klein,[38] who used sulfided hydrotreating catalysts; reaction networks, however, were either not reported or limited to few products. Adjaye and Bakhshi,[12,14,34] Hurff and Klein,[38] Samolada et al.,[17] Sharma and Bakhshi,[6−10] and Elliott et al.[15] reported mass balance closures, but others have not.

The following paper is part of a series[39−42] concerned with various bio-oil compounds; early results for anisole have been communicated.[39] We now report details, which include mass balances, selectivity-conversion plots with error bounds, rate constants of product formation, and a quantitative reaction network, characterizing the conversion of anisole catalyzed by a supported metal, Pt/Al_2O_3, in the presence of H_2. We also report the design of a reactor system that includes the capability for extensive online analysis of gas products by gas chromatography

Received: July 21, 2011
Revised: August 25, 2011
Published: August 28, 2011

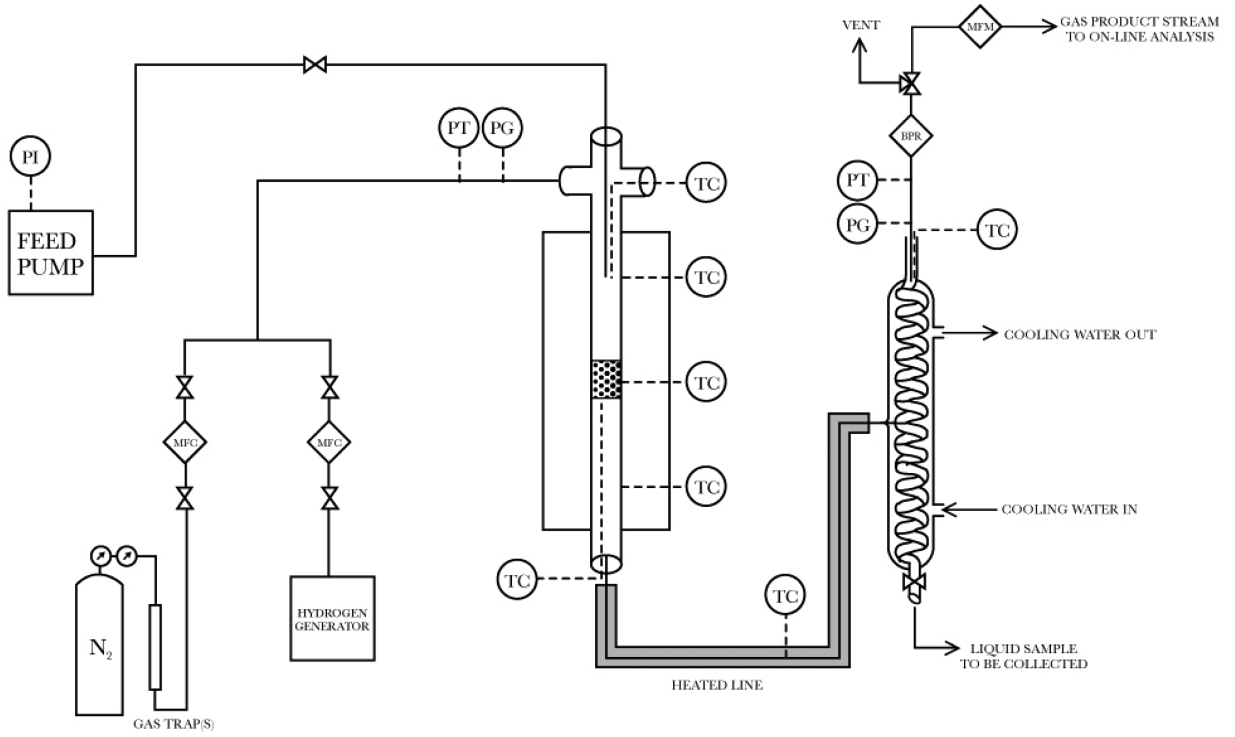

Figure 1. Schematic representation of once-through, packed-bed flow reactor system. Abbreviations: TC, thermocouple; PI, pressure indicator; PT, pressure transducer; PG, analogue pressure gauge; BPR, back-pressure regulator; MFM, mass flow meter; MFC, mass flow controller.

and at-line analysis of liquid products by gas chromatography with identification of products by gas chromatography/mass spectrometry; we have used this system to evaluate reaction products and establish the reaction network.

EXPERIMENTAL METHODS

Materials. Anisole (methoxybenzene, 99.8%) was purchased from Sigma-Aldrich. Pt/γ-Al_2O_3 powder (<100 mesh) containing 1 wt % Pt was acquired from Sigma-Aldrich. N_2 (99.997%, from Praxair), further purified by passage through a BHT-4 hydrocarbon trap (Agilent Technologies) to remove traces of hydrocarbon, was used as an inert carrier gas in the gas−solid reaction system and in the gas chromatographs. H_2 (99.999%), generated from deionized water by electrolysis in a model 40H gas generator (Domnick Hunter), was used as a reactant in the catalytic conversion experiments and in the gas chromatographs. Helium (99.995%, Praxair) was purified by passage through a BHT-4 trap (Agilent Technologies) to remove traces of hydrocarbon, a BMT-4 trap (Agilent Technologies) to remove moisture, and a BOT-4 trap (Agilent Technologies) to remove oxygen prior to use in the gas chromatographs. Zero-air (<0.1 ppm hydrocarbon (as methane)) was generated from house air in a model UHP-10ZAW zero air generator (Domnick Hunter) and was used in the gas chromatograph flame ionization detectors. The BET surface area of the catalyst was measured with a Micromeritics ASAP 2020 instrument, and the dispersion of the platinum in the catalyst was measured with a Micromeritics Autochem II Chemisorption Analyzer.

Flow Reactor System. Catalytic reaction experiments were carried out with a once-through packed-bed flow reactor (316 L stainless steel, O.D. = 0.5 in., wall thickness = 0.035 in.). A schematic diagram of the flow system is shown in Figure 1.

The liquid reactant was preloaded at room temperature into a syringe pump (Model 500D, Teledyne-ISCO), which was used as a liquid feed reservoir. Mass flow controllers (Model SLA5850S, Brooks Instruments) were used to measure and control gas flow rates. N_2 was used as the carrier gas. H_2, when used as a reactant, was mixed into the carrier gas stream via a Swagelok union cross (4-way) downstream of the mass flow controllers. The gas stream was mixed with vaporized anisole reactant at the inlet of the reactor in the top zone of a three-zone furnace. At the top of the downflow reactor, a Swagelok union cross provided three inlets to the reactor, one for gases, one for liquid fed through a capillary tube (stainless steel, O.D. = 1/16 in., I.D. = 0.020 in., Model U-104, Upchurch Scientific), and one for a thermocouple (Model HKMTSS-040U-12, Omega Engineering), which was placed near the tip of the capillary tube to measure the temperature of vaporization of the liquid feed. From the outlet of the reactor, the product stream flowed through a Swagelok (3-way) union tee, which also allowed mounting of a thermocouple (Model KQSS-116U-18, Omega Engineering) inside the reactor immediately downstream of the packed bed.

The reactor was mounted in a three-zone furnace (Series 3210, Applied Test Systems), which was designed for precise temperature control. Five thermocouples were used to measure temperatures inside (at the two locations mentioned above) and outside the reactor. The temperatures of the vaporization zone and packed bed were controlled by using the measurements of temperature determined with thermocouples in the reactor. Thermocouple wells extending axially into each zone of the furnace enabled positioning of thermocouples near the outer wall of the reactor and monitoring of temperatures in each zone at the outer reactor wall. The temperature of the zone downstream of the packed bed was controlled by using the signal of the thermocouple mounted at the outside wall of the reactor. The temperatures of the three heating zones were controlled separately.

The packed bed, holding 4.1−401.5 mg of catalyst particles, was typically 10 to 30 mm long. Glass wool and the packed bed of catalyst particles were positioned at the midpoint of the reactor and furnace. To provide nearly flat radial velocity and temperature profiles in the bed, the catalyst particles were mixed with particles of inert α-Al_2O_3 (A634-3 alundum, Fisher, 90 mesh particle size).

dx.doi.org/10.1021/ef2010699 |*Energy Fuels* 2011, 25, 4776–4785

After exiting the reactor, the product stream flowed through stainless steel tubing that was heated by electrical heating tape (HTC-120, Omega), extending from the exit of the reactor to the inlet of a condenser. Water at approximately 10 °C was used as a coolant, and the outlet gas stream exited the condenser at approximately 12 °C, as measured by a thermocouple (KQMSS-020G-6, Omega). Liquid samples were collected at intervals of approximately 20 min from the bottom of the condenser and weighed. The flow rate of the gas product stream was monitored with a SLA 7860S mass flow meter (Brooks Instruments).

Safety features enabled redundant monitoring of key control points. For instance, both pressure transducers (PTI-S-NG250-22AQ, Swagelok) and analogue pressure gauges (PGI-63B-PG200-LAQX-J, Swagelok) were placed upstream of the reactor and downstream of the condenser; the pressure in the system was controlled by a manual back-pressure regulator (44-2300 Series, Tescom). Reactor temperatures were measured in each zone, both inside and outside of the reactor; upper limits were included in the control program for automatic shut-off of power to the furnace.

Product Analysis. Analysis of the products in the liquid samples was performed with an Agilent 7890A gas chromatograph (GC) equipped with a 5975C mass selective detector (MSD) incorporating a quadrupole mass analyzer. Analyte separation was achieved with a DB-624 Agilent J&W column (0.25 mm/60 m/1.4 μm) with 2.4 mL/min helium carrier gas flow rate and a temperature ramp program. Peaks were identified by using the Agilent quality match factor (Qual), which is based on how well the ion ratios match those of the NIST EI mass spectral library database standard; each compound except water and methanol scored greater than 90. Retention times of some of the compounds were confirmed by use of calibration samples. Product quantification was carried out with an Agilent 7890A GC using a flame ionization detector (FID); analyte separation was achieved with a DB-624 Agilent J&W column (0.25 mm/60 m/1.4 μm). The operating parameters of the GC-FID were developed to obtain essentially the same peak retention times and separations as with the GC-MSD. The FID was operated at 300 mL/min zero-air and 25 mL/min H_2 flow rates. Calibration curves, each with at least five points, were used to quantify the following products: benzene, cyclohexanone, phenol, 2-methylanisole, 4-methylanisole, 2-methylphenol, 4-methylphenol, and 2,6-dimethylphenol. Other products were analyzed semiquantitatively on the basis of results obtained for chemically similar components (containing the same numbers of carbon and oxygen atoms).

A GC (Agilent 7890A), equipped with three sample loops, five columns, and three detectors (one FID and two TC detectors), was used to analyze the gas effluent from the condenser. Each of the sample loops was 500 μL in volume. Hydrocarbons were separated in an HP-Al/S (19095P-S25, 50 m long/0.53 mm in I.D./15 μm in film thickness) Agilent J&W capillary column with a helium carrier gas flow rate of 27 mL/min, and the components were quantified by analysis with an FID. The FID was operated at 300 mL/min zero-air and 25 mL/min H_2 flow rates. Fixed gases and methane were separated with three Agilent 1/8-in stainless-steel packed columns mounted in series: HayeSep Q (6 ft), HayeSep N (8 ft), and Molsieve 13X (10 ft), and the components were quantified with a TCD with helium carrier gas at a pressure of 70 kPa. H_2 was separated in a 4-ft Molsieve 13X packed column and quantified with a TCD using N_2 carrier gas. Temperature and carrier gas flow ramps were used to improve the retention time and separation of compounds. Gas samples were taken online at approximately 30 min intervals; each of the sample loops was actuated, nearly simultaneously, to load the flow paths to each of the detectors and to characterize the gas stream. Peak identification was carried out by comparison with a NIST traceable Agilent Technologies/Praxair RGA gas calibration standard (5184-3545, Lot No. 091509R). Single-point calibrations, determined using data collected with compounds (listed in the Supporting Information, SI Table 1) in the gas calibration standard, were used to quantify products in the gas stream.

Catalyst Loading, Preparation, and Testing. The Pt/Al_2O_3 catalyst was held in place in the reactor with approximately 0.1 g of quartz wool mounted near the axial center of the reactor. A bed of approximately 2 g of α-Al_2O_3 was placed on the quartz wool; downstream of it was a bed of catalyst particles mixed with 1−2 g of α-Al_2O_3, and upstream of that was another bed of 2 g of α-Al_2O_3 particles. The catalyst was heated in N_2 flowing at 70 mL/min at NTP and H_2 (flowing at a rate of 30 mL/min at NTP) at a rate of 5 °C/min to 573 K and held at this temperature for 30 min prior to the start of reactant flow. The catalyst mass was in the range of 4.1−401.5 mg.

The catalytic conversion of anisole was carried out at 573 K and approximately 140 kPa; the anisole flow rate was 0.03 mL/min, and the N_2 and H_2 flow rates were 70 and 30 mL(NTP)/min, respectively. The range of the weight hourly space velocity (WHSV) was 17.6−437 (g of anisole)/(g of catalyst × h), varied by changing the catalyst mass. Fresh catalyst was used for each experiment. Experiments were typically run for 6 h time-on-stream.

Data Analysis. Conversions of anisole were determined on the basis of mass balance calculations for the reaction system. The terms in the mass balance included the flow rate of anisole into the reactor and the flow rates of the liquid condensate and gas streams out of the condenser; the mass of the packed bed was measured before and after each experiment to allow a determination of the accumulation of mass in it. The mass of reactant entering the reactor was calculated from the volumetric flow rate and density of the reactant (flowing at approximately NTP). The mass of liquid condensate was determined periodically by measuring the mass of liquid collected in each vial and summing over the samples. The mass of the reactant leaving the condenser in the gas phase was calculated from the flow rate of the gas and by using an Antoine vapor pressure correlation and assuming that the inert gas was saturated with the reactant at the exit temperature of the condenser. Because the condenser did not drain perfectly, the mass of liquid remaining in the condenser at the end of each experiment was determined from the mass of liquid fed into the system prior to the collection of liquid at the bottom of the condenser.

Conversions (X) were calculated as the molar flow rates of anisole reactant consumed divided by the total molar flow rate of anisole fed. The mass of products, taken to be the mass of reactant consumed, was determined by quantifying GC-FID peak areas. The number of moles of reactant consumed in any experiment was calculated from the mass of reactant consumed and the molecular weight of the reactant. Selectivity is defined here as the molar flow rate of product divided by molar flow rate of reactant consumed. Yield is defined here as conversion times selectivity.

Initial conversion data were obtained by extrapolating the conversion vs time-on-stream data to zero time on stream by using a linear fit. These initial conversion data were used to find the fraction of anisole reactant unconverted as a function of inverse WHSV, as well as yield as a function of conversion and selectivity as a function of conversion.

Identification of Primary and Nonprimary Products. Selectivity vs. conversion plots were used to determine which products were primary and which were nonprimary, on the basis of the ordinate-intercepts of the linear regression line through the data points; data that determine an ordinate axis intercept of the regression line significantly different from zero (with 95% confidence limits) are considered to be indicative of primary products.[43,44]

Determination of Reaction Rates from Differential Conversion Data. Data were plotted to demonstrate that some conversions were differential. The pseudo-first-order rate constant for the overall disappearance of anisole was determined from a semilogarithmic plot of fraction of reactant unconverted, $(1 - X)$, as a function of inverse WHSV. The pseudo-first-order rate constants for the production of primary products were determined from plots of conversion vs inverse space velocity.

Table 1. Overall Mass Balance Closure Data[a]

experiment number	mass balance closure (%)	time on stream (min)	mass of liquid fed[b] (g)	mass of liquid collected from condenser[b] (g)	mass of reactant leaving condenser as vapor[b] (g)	mass of liquid remaining in condenser (g), estimated
1	94.7	347	10.4	9.04	0.26	0.5
2	99.5	286	8.56	7.62	0.20	0.5
3	99.8	403	12.0	11.2	0.34	0.5
4	98.9	382	11.4	10.5	0.32	0.5
5	99.2	358	10.7	9.81	0.30	0.5
6	100.5	381	11.4	10.7	0.32	0.5
7	101.0	170	5.06	4.47	0.14	0.5

[a] The data in each row represent results from an individual experiment. [b] The data showing liquid fed, liquid collected from condenser, and reactant leaving the condenser in the vapor phase are cumulative values for the length of the experiment.

RESULTS

Catalyst Physical Properties. The BET surface area of the catalyst was found to be 206 ± 1 m^2/g, and the dispersion of the platinum was found to be approximately 0.25.

Mass Balance Closures. Mass balance closures were typically 99.5 ± 1.0% (and they were generally greater than 95%) in experiments with anisole conversions up to 17% (Table 1). The reactant and most products have low vapor pressures at the exit temperature of the condenser, and we, therefore, infer that they were almost completely condensed. The mass of reactant leaving the condenser in the vapor phase was determined to be between 2.5 and 2.8% of the mass fed into the reactor, and it is accounted for in the mass balance calculation (Table 1). The contributions of the products exiting the condenser in the vapor phase, which generally have lower vapor pressures at the temperature of the condenser, constitute a negligible contribution to the overall mass balance. As a result, mass balance closures were not significantly different from 100% even when a quantitative accounting for products exiting the condenser in the gas phase was omitted. The changes in mass of the packed bed were negligible relative to other terms in the mass balance and did not contribute significantly to the overall mass balance.

Major, Minor, and Trace Products of Anisole Conversion. Dozens of products were identified in the conversion of anisole catalyzed by Pt/Al_2O_3. Data were obtained at conversions as low as 0.01 to determine primary reactions and the associated kinetics parameters. Product formation data were also obtained at higher conversions, up to $X = 0.2$, to identify nonprimary products. As a control, experiments were performed using a bed of only α-Al_2O_3 (without catalyst); essentially no conversion ($X < 0.001$) was observed under these conditions.

The most abundant compounds identified at an anisole conversion of approximately 0.2 are listed in Table 2. The major products include methane, benzene, cyclohexanone, 2-methylphenol, 2-methylanisole, phenol, and 2,6-dimethylphenol. The conversions to these products were determined quantitatively. Other products formed in relatively high yields include 4-methylphenol, methoxycyclohexane, and 4-methylanisole. Water and methanol were products observed by GC-MS but not quantified. Trace products (identified only qualitatively) included methylcyclohexanone, cyclohexane, methylcyclohexane, 1,1-dimethylcyclohexane, *o*-xylene, *p*-xylene, 2,6-dimethylanisole, 2,4-dimethylphenol, and trimethylphenol.

Conversion of Anisole as a Function of Time on Stream and of Inverse Space Velocity. The conversion of anisole catalyzed by Pt/Al_2O_3 as a function of time on stream at various space velocities is shown in Figure 2. These data demonstrate catalyst deactivation. In a typical experiment, the deactivation led to a decline in conversion of about 50% in 6 h. The yields of various products vs time on stream do not suggest that deactivation affects a particular reaction class more strongly than the others. Initial conversions were determined by extrapolating the data to zero time on stream. Error bars on the data are shown for experiments carried out with a WHSV of 34 (g of reactant)/(g of catalyst × h). The data indicate that higher space velocities lead to lower initial conversions, as expected.

Development of a Quantitative Reaction Network. Plots of selectivity (molar flow rate of product divided by molar flow rate of reactant consumed) as a function of conversion were used to identify which products were primary and which were not.[43,44] Data for each product were fitted with a straight line and extrapolated to zero conversion; intercepts of linear regression lines significantly different from zero selectivity at zero conversion (determined with 95% confidence limits) indicate primary products. The selectivity-conversion data observed for anisole (Figure 3) indicate that phenol, 2-methylphenol, 4-methylphenol, 2-methylanisole, and 2,6-dimethylphenol were primary products and that benzene and cyclohexanone were higher-order products. We infer, however, that 2,6-dimethyl phenol was produced from anisole by a sequence of reactions and, in small quantities, from feed impurities (<0.2%) such as methylphenols.

The first step in the determination of a reaction network is to infer the likely reaction classes from the identities of the products. Thus, analysis of the products can give an indication of the reaction classes in the conversion of anisole catalyzed by Pt/Al_2O_3.

The most abundant products point to the following important (i.e., kinetically significant) reaction classes: hydrogenolysis (indicated, for example, by the formation of phenol and methane), hydrodeoxygenation (indicated, for example, by the formation of benzene), hydrogenation (indicated, for example, by the formation of cyclohexanone), and methyl group transfer (transalkylation) (indicated, for example, by the formation of 2-methylphenol).

We infer that phenol is formed in both hydrogenolysis and transalkylation reactions; other major products, including 2-methylanisole and 2-methylphenol, likely result from single methyl group transfer reactions. 2,6-Dimethylphenol is inferred to have been formed in sequential transalkylation reactions. Methanol and benzene are inferred to have been formed by hydrogenolysis of the C−O bond, referred to here as hydrodeoxygenation. Cyclohexanone is inferred to have been formed by a sequence of reactions: removal of the methyl group bonded

Table 2. Most Abundant Products and Trace Products Formed in the Conversion[a] of Anisole Catalyzed by Pt/Al_2O_3 (Compounds Identified in Liquid Product)[b]

product	classification based on abundance in product stream	basis for identification of product	basis for quantification of product
benzene	major	comparison of GC trace with that of standard sample	FID calibration curve
methoxycyclohexane	minor	MS EI database	n/a
cyclohexanone	major	comparison of GC trace with that of standard sample	FID calibration curve
2-methylanisole	major	comparison of GC trace with that of standard sample	FID calibration curve
4-methylanisole	minor	comparison of GC trace with that of standard sample	n/a
phenol	major	comparison of GC trace with that of standard sample	FID calibration curve
2-methylphenol	major	comparison of GC trace with that of standard sample	FID calibration curve
4-methylphenol	minor	comparison of GC trace with that of standard sample	n/a
2,6-dimethylphenol	major	comparison of GC trace with that of standard sample	FID calibration curve
cyclohexane	trace	comparison of GC trace with that of standard sample	n/a
methylcyclohexane	trace	MS EI database	n/a
1,1 dimethylcyclohexane	trace	MS EI database	n/a
p-xylene	trace	MS EI database	n/a
o-xylene	trace	MS EI database	n/a
2-methylcyclohexanone	trace	MS EI database	n/a
2,6-dimethylanisole	trace	MS EI database	n/a
2,4-dimethylphenol	trace	MS EI database	n/a
trimethylphenol	trace	MS EI database	n/a
water	n/a	MS EI database	n/a
methanol[c]	n/a	MS EI database	n/a

[a] Conversion conditions: temperature, 573 K; WHSV, 4.46 (g of reactant)/(g of catalyst × h); initial conversion of anisole was approximately 0.2. The retention times of the compounds identified in the liquid samples were consistent with the retention times of the compounds determined in experiments with authentic calibration samples. [b] Compounds were identified with the NIST EI mass spectral database and by requiring that the Agilent quality match factor (Qual) score be greater than 90; other isomers, for example, other dimethylanisole isomers, are possible. Some compounds were confirmed by comparison with a GC trace characterizing standard samples. [c] Methanol was observed in liquid samples; its concentration in the gas phase was not quantified.

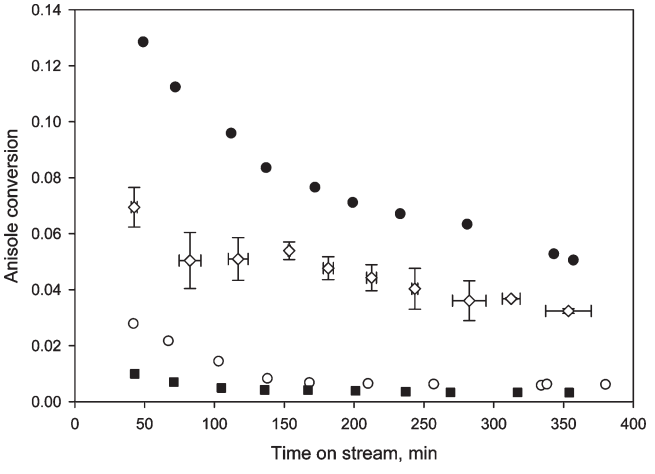

Figure 2. Change in anisole conversion during operation of a flow reactor at 573 K and at various values of WHSV (WHSV in units of (g of reactant)/(g of catalyst × h)): 18 (●), 34 (◇), 150 (○), and 440 (■). An average of duplicate values is shown for WHSV = 34 (g of reactant)/(g of catalyst × h).

to oxygen by hydrogenolysis or dealkylation and hydrogenation of the aromatic ring.

Transalkylation reactions are inferred to have produced the minor products 4-methylphenol and 4-methylanisole. Sequential hydrogenation reactions of the aromatic ring are inferred to have produced methoxycyclohexane.

The trace products are inferred to have been formed by sequential reactions. These products can be accounted for by the following reaction classes: transalkylation and hydrogenation of the aromatic ring, leading to methylcyclohexanone, and hydrodeoxygenation, hydrogenation, and transalkylation, accounting for cyclohexane and methylcyclohexane. Multiple transalkylation reactions account for methylphenols and methylanisoles with multiple methyl substituents (e.g., various dimethylphenol isomers and dimethylanisole isomers).

A partial statement of the reaction network, representing just the primary products and other important products, is shown in Figure 4. According to this representation, hydrogenolysis, methyl group transfer, hydrodeoxygenation, and hydrogenation are the kinetically significant reaction classes in the anisole conversion catalyzed by Pt/Al_2O_3 in the presence of H_2. Specifically, methyl group transfer to methylphenols produced dimethylphenols, which we infer eventually led to trimethylphenols and tetramethylphenols. Methylbenzene (toluene) could be produced from either methylphenol or methylanisole by hydrodeoxygenation reactions, which also lead to the formation of benzene from phenol or anisole.

The data allow a quantitative characterization of the overall conversion of anisole catalyzed by Pt/Al_2O_3. The overall anisole conversion is well represented by first-order kinetics (Figure 5). The pseudo-first-order rate constant for the disappearance of anisole was found to be 19 L/(g of catalyst × h) under the conditions stated in the caption of Figure 2. Using estimates of

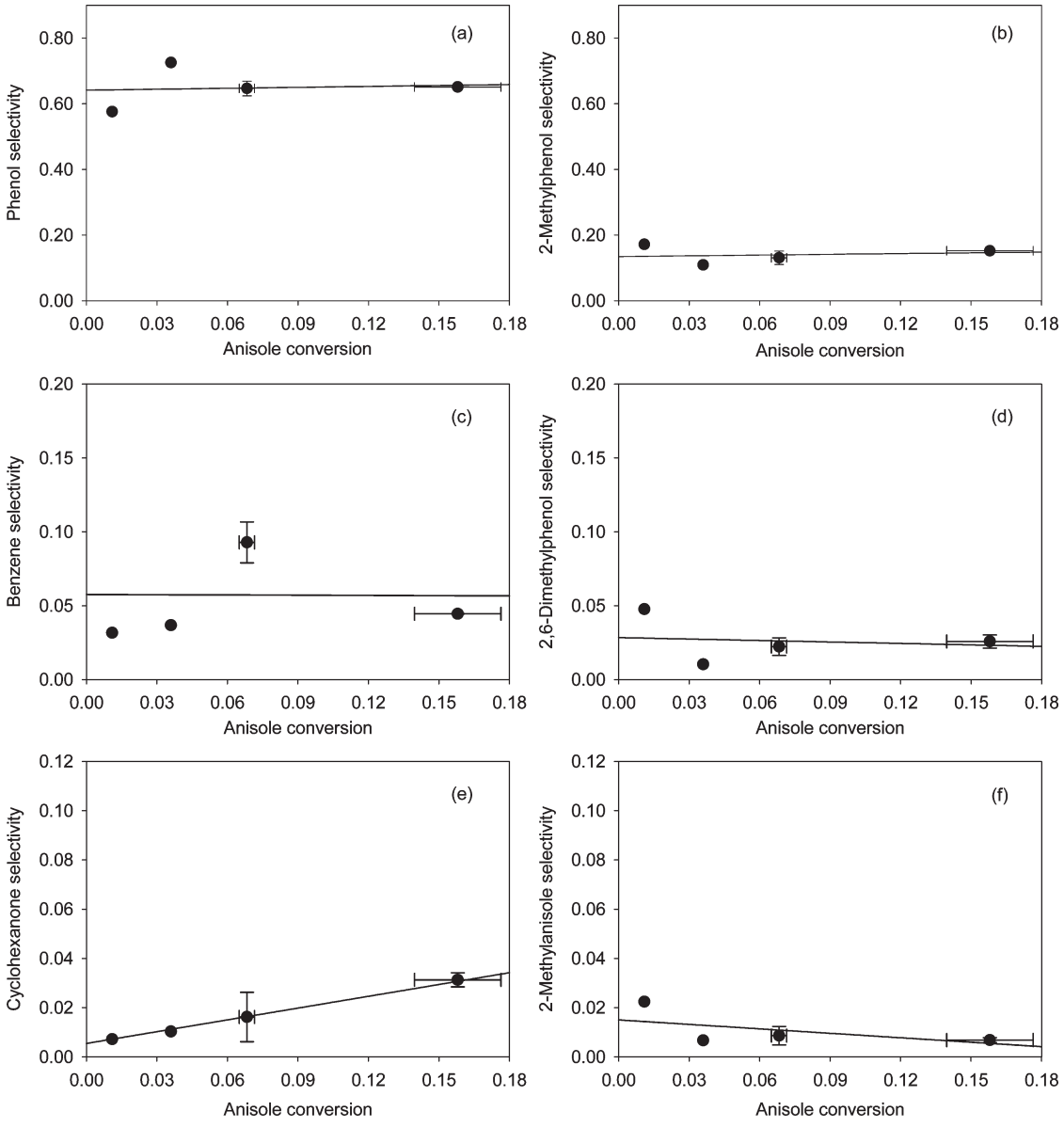

Figure 3. Selectivity for the formation of several products in the conversion of anisole catalyzed by Pt/Al_2O_3 in the presence of H_2 at 573 K; error bars were determined in replicate experiments at conversions of approximately 0.07 and 0.16. Data for each product were fitted with a straight line and extrapolated to zero conversion; intercepts of regression lines significantly different from zero selectivity at zero conversion (analyzed with 95% confidence limits) indicate primary products. Primary products in this case are phenol (a), 2-methylphenol (b), 2-methylanisole (f), and 2,6-dimethylphenol (d), and those with intercepts not significantly different from zero (determined with 95% confidence limits) are considered to be evidence of higher-order products, in this case benzene (c) and cyclohexanone (e). The selectivity-conversion plot for 4-methylphenol (ESI Figure 1) indicates that it is a primary product.

the diameter and density of catalyst particles, the average diameter of the catalyst pores, and the reactant diffusivity, we judged on the basis of the Weisz-Prater criterion, assuming spherical particles and first-order kinetics, that influence of intraparticle mass transport was negligible.

Data characterizing the formation of some of the products are also well represented by first-order kinetics. The results (Figure 6) allow the partially quantified statement of the reaction network shown in Figure 4, which includes the pseudo-first-order rate constants for each of the reactions, for example, the methyl group transfer that results in the formation of 2-methylphenol from anisole. The pseudo-first-order rate constants for the formation of these products are summarized in Figure 4.

The product that formed fastest from anisole was phenol. This product was formed more than four times faster than 2-methylphenol, and the other products were formed even more slowly. The formation of 2-methylanisole was an order of magnitude slower than the formation of 2-methylphenol. The formation of 4-methylphenol was nearly 2 orders of magnitude slower than the formation of 2-methylphenol, which indicates a kinetic preference for the substitution at the *ortho* position. Each of the products is possibly formed by a single reaction; however, these products could also be formed by sequences of reactions.

In contrast, we infer that 2,6-dimethylphenol was formed only in a sequence of methyl-group transfers. The primary product, for instance, can be inferred to be 2-methylphenol or 2-methylanisole.

dx.doi.org/10.1021/ef2010699 |*Energy Fuels* 2011, 25, 4776–4785

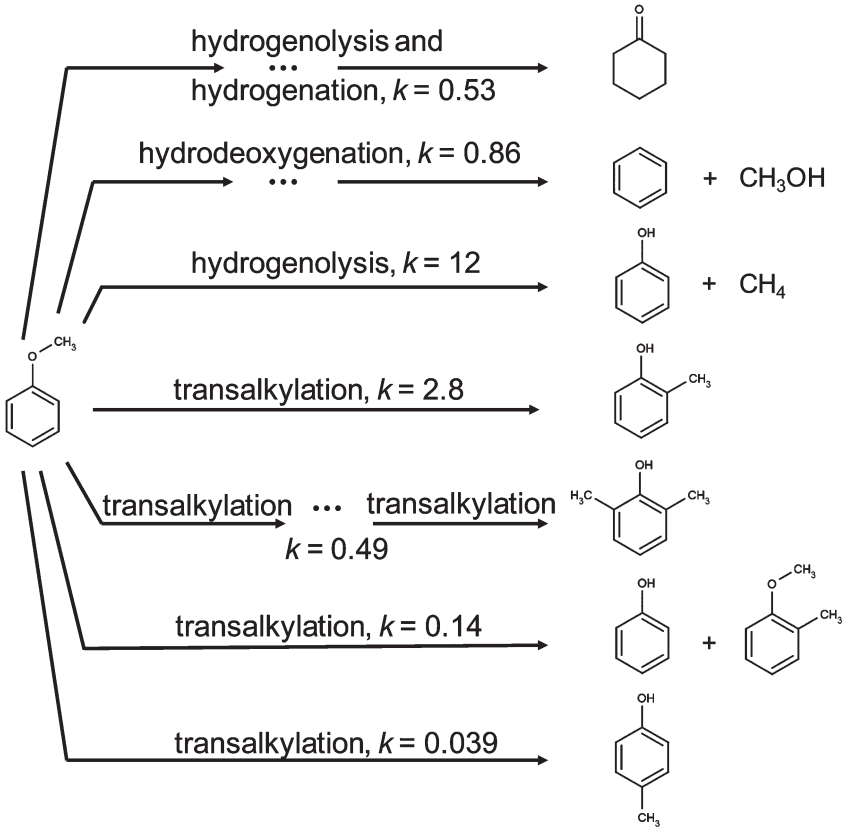

Figure 4. Reaction network to primary products and to other important products based on analysis of selectivity-conversion plots for the conversion of anisole and H_2 catalyzed by Pt/Al_2O_3 at 573 K. H_2, as a reactant, is omitted for simplicity. 2,6-Dimethylphenol appears (on the basis of the selectivity-conversion plot) to be a primary product, but we infer that it must have been formed by a sequence of reactions. Pseudo-first-order rate constants for the individual primary products formed in the conversion of anisole catalyzed by Pt/Al_2O_3 are in units of L/(g of catalyst × h). The reaction temperature was 573 K. These rate constants were determined from the conversions to the individual products, which, for example, in the case of phenol, may be formed in more than one reaction pathway, as shown here.

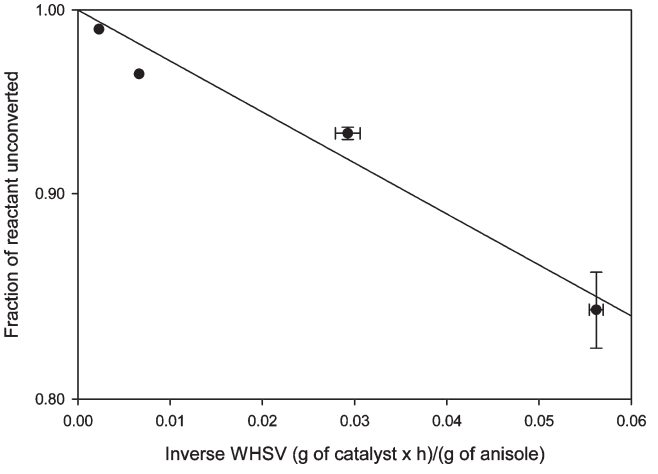

Figure 5. Demonstration of first-order kinetics of overall conversion of anisole catalyzed by Pt/Al_2O_3 under the conditions stated in the text. Error bars of replicates are shown at inverse WHSV = 0.056 and 0.029 (g of catalyst × h)/(g of anisole).

The formation of benzene and of cyclohexanone, although they are evidently not primary products, is in each case adequately represented by first-order kinetics (Figure 7). The pseudo-first-order rate constant characterizing benzene formation was determined to be $k = 0.86$ L/(g of catalyst × h), and that found for cyclohexanone formation was $k = 0.53$ L/(g of catalyst × h).

Presuming that methyl group transfer, hydrodeoxygenation, hydrogenolysis, and hydrogenation are the important reaction classes and by recognizing which compounds were primary products and which were not, we inferred the more extensive reaction network of Figure 8. As this network shows, most of the products in the conversion of anisole were likely formed in sequential reactions; they were not primary products. However, the data are not sufficient to fully elucidate the nonprimary products.

The data are not sufficient to identify all of the primary reactions. For example, phenol could have been formed as a primary product via several pathways, each with a different coproduct: methane, 2-methylanisole, and 4-methylanisole. Because the selectivity for formation of neither 2-methylanisole nor 4-methylanisole matches that of phenol, we infer that the primary pathway for phenol formation is hydrogenolysis of anisole (to give phenol and methane).

2-Methylphenol, as well as 4-methylphenol, can also be formed via multiple pathways: intramolecular transalkylation of anisole or intermolecular transalkylation involving phenol and anisole. The further addition of methyl substituents to the aromatic ring to produce dimethylphenols, trimethylphenols, and so forth allows for a number of possible pathways. 2-Methylanisole and 4-methylanisole are inferred to be formed primarily from single methyl group transfer reactions.

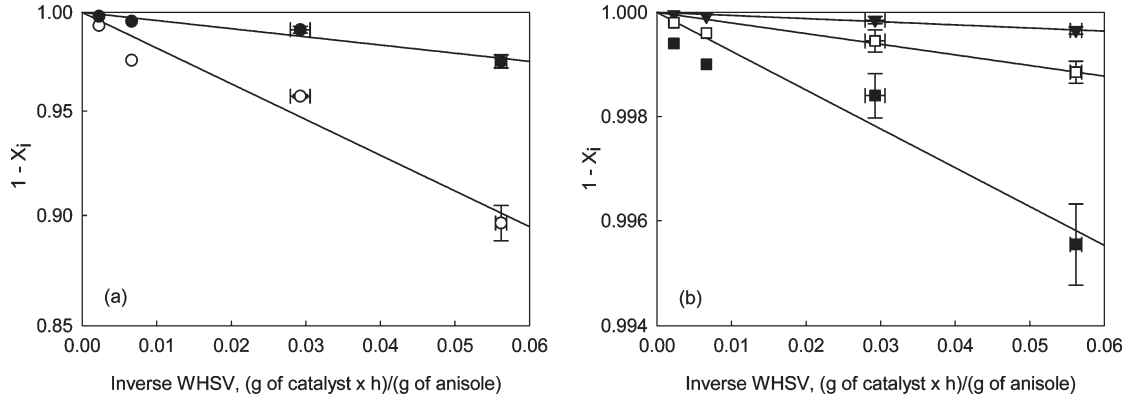

Figure 6. Semilogarithmic plots of the conversion of anisole in the presence of H_2 to give phenol (○), 2-methylphenol (●), 2,6-dimethylphenol (□), 2-methylanisole (■), and 4-methylphenol (▼) at 573 K. The term $(1 - X_i)$ represents the conversion to product *i*. Conversion was varied by changing the catalyst mass in the packed bed.

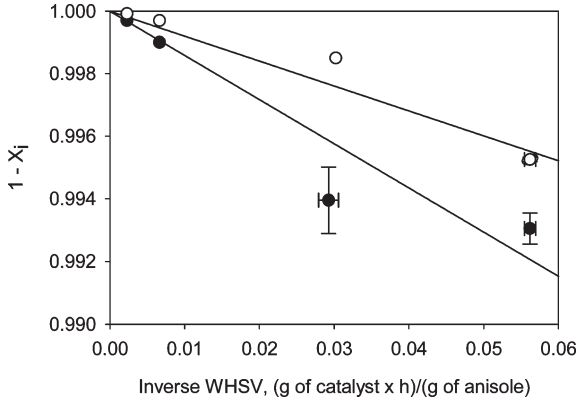

Figure 7. Semilogarithmic plots of the conversion of anisole in the presence of H_2 to give cyclohexanone (○) and benzene (●) at 573 K. The term $(1 - X_i)$ represents the conversion of anisole to product *i*. Conversion was varied by changing the catalyst mass in the packed bed.

Benzene was also possibly formed via parallel pathways, both involving hydrodeoxygenation. From the (qualitative) observation of methanol, we infer that hydrodeoxygenation of anisole produces methanol and benzene. Hydrodeoxygenation of phenol can also produce benzene and water. Hydrogenation of phenol has been shown to produce cyclohexanone.[45,46] These reactions with hydrogen likely occurred with methyl-substituted phenols and anisoles to form methyl-substituted benzenes.

In summary, the reaction network of Figure 8 accounts for our data and accounts for the kinetically important reaction classes, but we recognize that it is an approximation that could be improved with the availability of more extensive data.

■ DISCUSSION

The catalytic conversion of anisole catalyzed by platinum supported on γ-Al_2O_3, an acidic support, shows some similarity to anisole conversion catalyzed by solid acids without noble metals. For example, Chantal et al.,[32] using HZSM-5 as a catalyst, observed high yields of phenol, methylphenols, and dimethylphenols at 623 K with a residence time in a plug-flow reactor of 0.83 h. Using HZSM-5 as a catalyst, Zhu et al.[35] observed the formation of phenol, methylphenols, and methylanisoles in high yields at 673 K and over a range of residence times in a plug-flow reactor ranging from less than 0.05 to 1.0 h. For comparison, our residence times ranged from 2.3×10^{-3} to 56.7×10^{-3} h.

In their experiments with acidic catalysts, Chantal et al.[32] and Zhu et al.[35] also observed the removal of oxygen from anisole and the formation of aromatic products. The highest selectivity to aromatics indicated by their data was 0.05,[32] which is lower than our observed selectivity to benzene of almost 0.10. Chantal et al.[32] and Zhu et al.[35] used higher temperatures and higher average residence times than ours, and we suggest that the differences in severity between their conditions and ours account in part for the different product distributions, but we attribute the differences primarily to the presence of the noble metal in our catalyst and the lack of such a metal in theirs.

In experiments with a bifunctional hydrotreating catalyst, sulfided Ni−Mo/SiO_2−Al_2O_3, which contains an acidic support, Bredenberg et al.[37] also observed the formation of methylphenols and methylanisole in the conversion of anisole at 573 K. They also reported a selectivity for benzene formation of 0.055 at an anisole conversion of 0.76. The data cannot be directly compared with ours, which are characterized by a maximum observed selectivity for benzene formation of 0.10, because the conversions are dramatically different. The conversion and yield data reported by Hurff and Klein[38] indicate a selectivity for benzene formation at high conversion similar to that of Bredenberg et al.,[37] although a precise value cannot be estimated at low conversions because of the scale of the plot in the publication.[38]

Thus, the routes by which oxygen was removed from anisole in the reported acid-catalyzed reactions are not clear from the information presented by the authors. We emphasize that in our case we attribute the oxygen removal largely to the role of platinum in activating H_2 for hydrodeoxygenation reactions. There are numerous examples of similar reactions catalyzed by noble metals, exemplified the hydrodeoxygenation of guaiacol catalyzed by rhodium, palladium, and platinum supported on zirconia.[47] Ours is evidently the first report of the hydrodeoxygenation of anisole catalyzed by a supported noble metal.

Hydroprocessing catalysts incorporating metals such as molybdenum have also been used for hydrodeoxygenation. For example, Hurff and Klein[38] and Bredenberg et al.[37] used sulfided CoMo/γ-Al_2O_3 for removal of oxygen from anisole, observing benzene as a major product at high conversions in a batch reactor; the benzene was evidently formed from phenol, which was a major primary product according to their reaction network.

dx.doi.org/10.1021/ef2010699 |*Energy Fuels* 2011, 25, 4776–4785

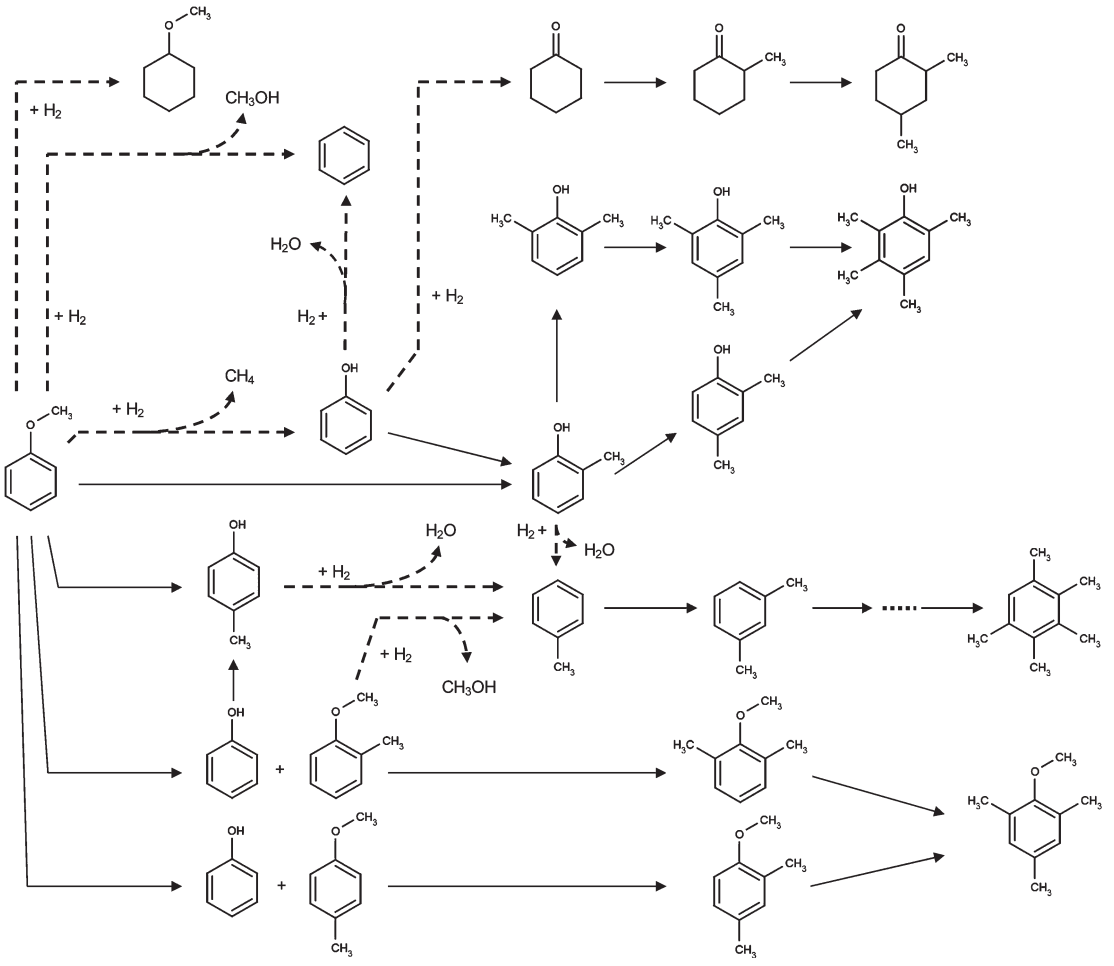

Figure 8. Reaction network for the conversion of anisole and H_2 catalyzed by Pt/Al_2O_3 at 573 K. Hydrodeoxygenation, hydrogenolysis, and hydrogenation reactions are represented by dashed arrows, and methyl group transfer reactions are represented by solid arrows.

In contrast, our results show the catalytic formation of benzene at relatively low conversions of anisole, consistent with the catalytic role of the platinum.

CONCLUSIONS

In comparison with the work of earlier investigators who considered catalytic anisole conversion, we have been able to develop a more extensive reaction network, including quantification of rates of formation of primary products. The data enable us to infer relative contributions of the various reaction classes. We infer the platinum catalyzed hydrogenolysis of the anisole to produce methane and phenol, which is a kinetically significant reaction under our conditions. All other primary products were apparently produced by methyl group transfer reactions. Higher-order products that were observed in relatively high yields include benzene, formed by hydrodeoxygenation of anisole or phenol, and cyclohexanone, formed by hydrogenation of phenol. We infer that reactions in both of these classes were catalyzed by the platinum. Methyl group transfer apparently catalyzed the formation of numerous higher-order products such as dimethylanisoles, trimethylphenols, and pentamethylbenzenes, formed, for example, from methylanisole and anisole, dimethylphenol and anisole, and tetramethylbenzene and anisole, respectively.

Although the reaction network could be elucidated in more detail than we have presented, with the benefit of additional data (such as could be obtained with intermediates in the feed stream), an important practical inference that is already clear on the basis of our results is that selective oxygen removal from compounds such as anisole may require both (a) catalysts with functions that are active for hydrodeoxygenation (such as noble metals) and (b) substantially higher H_2 partial pressures than we have investigated in this work.

ASSOCIATED CONTENT

Supporting Information. Table containing the composition of the gas calibration standard and a figure showing 4-methylphenol selectivity-conversion data. This material is available free of charge via the Internet at http://pubs.acs.org.

AUTHOR INFORMATION

Corresponding Author

*E-mail: bcgates@ucdavis.edu.

Present Addresses

[§]Argonne National Laboratory, Chemical Sciences and Engineering Division, 9700 South Cass Ave, CSE/205, Chicago, IL 60439, USA.

■ ACKNOWLEDGMENT

We thank Jennifer Heelan of the University of California, Davis, for her help with the analytical instrumentation and Professor Alexander Katz of the University of California, Berkeley, for providing access to instruments for determination of the catalyst physical properties. Support of this work was provided by Chevron Technology Ventures, a division of Chevron U.S.A., Inc. An Agilent Technologies Foundation Research Project Gift provided a GC7890 Refinery Gas Analyzer. T.N. thanks the Fulbright Foundation for an Open Competition scholarship.

■ REFERENCES

(1) Bridgwater, A. V.; Cottam, M. L. *Energy Fuels* **1992**, *6*, 113–120.
(2) Huber, G. W.; Iborra, S.; Corma, A. *Chem. Rev.* **2006**, *106*, 4044–4098.
(3) Stöcker, M. *Angew. Chem., Int. Ed.* **2008**, *47*, 9200–9211.
(4) Elliott, D. C. *Energy Fuels* **2007**, *21*, 1792–1815.
(5) Furimsky, E. *Appl. Catal., A: Gen.* **2000**, *199*, 147–190.
(6) Sharma, R. K.; Bakhshi, N. N. *Fuel Process. Technol.* **1991**, *27*, 113–130.
(7) Sharma, R. K.; Bakhshi, N. N. *Appl. Catal.* **1991**, *76*, 1–17.
(8) Sharma, R. K.; Bakhshi, N. N. *Bioresour. Technol.* **1991**, *35*, 57–66.
(9) Sharma, R. K.; Bakhshi, N. N. *Energy Fuels* **1993**, *7*, 306–314.
(10) Sharma, R. K.; Bakhshi, N. N. *Biomass Bioenergy* **1993**, *5*, 445–455.
(11) Vitolo, S.; Seggiani, M.; Frediani, P.; Ambrosini, G.; Politi, L. *Fuel* **1999**, *78*, 1147–1159.
(12) Adjaye, J. D.; Bakhshi, N. N. *Fuel Process. Technol.* **1995**, *45*, 161–183.
(13) Adjaye, J. D.; Bakhshi, N. N. *Fuel Process. Technol.* **1995**, *45*, 185–202.
(14) Adjaye, J. D.; Katikaneni, S. P. R.; Bakhshi, N. N. *Fuel Process. Technol.* **1996**, *48*, 115–143.
(15) Elliott, D. C.; Hart, T. R.; Neuenschwander, G. G.; Rotness, L. J.; Zacher, A. H. *Environ. Prog. Sustainable Energy* **2009**, *28*, 441–449.
(16) Gagnon, J.; Kaliaguine, S. *Ind. Eng. Chem. Res.* **1988**, *27*, 1783–1788.
(17) Samolada, M. C.; Baldauf, W.; Vasalos, I. A. *Fuel* **1998**, *77*, 1667–1675.
(18) Gevert, S. B.; Andersson, P. B. W.; Sandqvist, S. P.; Jaeraas, S. G.; Tokarz, M. T. *Energy Fuels* **1990**, *4*, 78–81.
(19) Gevert, B. S.; Otterstedt, J. E. *Biomass* **1987**, *13*, 105–115.
(20) Baker, E. G.; Elliott, D. C. *ACS Symp. Ser.* **1988**, *376*, 228–40.
(21) Elliott, D. C.; Neuenschwander, G. G. In *Developments in Thermochemical Biomass Conversion*; Bridgwater, A. V., Boocock, D. G. B., Eds.; Blackie Academic & Professional: London, 1997; Vol. 1, pp 611−621.
(22) Piskorz, J.; Majerski, P.; Radlein, D.; Scott, D. S. *Energy Fuels* **1989**, *3*, 723–726.
(23) Samolada, M. C.; Baldauf, W.; Vasalos, I. A. *Fuel* **1998**, *77*, 1667–1675.
(24) Gevert, B. S.; Otterstedt, J. E.; Massoth, F. E. *Appl. Catal.* **1987**, *31*, 119–131.
(25) Petrocelli, F. P.; Klein, M. T. *Pet. Sci. Technol.* **1987**, *5*, 25–62.
(26) Laurent, E.; Delmon, B. *Appl. Catal., A: Gen.* **1994**, *109*, 77–96.
(27) Centeno, A.; Laurent, E.; Delmon, B. *J. Catal.* **1995**, *154*, 288–298.
(28) Centeno, A.; David, O.; Vanbellinghen, C.; Maggi, R.; Delmon, B. In *Developments in Thermochemical Biomass Conversion*; Bridgwater, A. V., Boocock, D. G. B., Eds. Blackie Academic & Professional: London, 1997; Vol. 1, pp 589−601.
(29) Shabtai, J.; Nag, N. K.; Massoth, F. E. *J. Catal.* **1987**, *104*, 413–423.
(30) Bredenberg, J. B.; Huuska, M.; Toropainen, P. *J. Catal.* **1989**, *120*, 401–408.
(31) Kallury, R. K. M. R.; Restivo, W. M.; Tidwell, T. T.; Boocock, D. G. B.; Crimi, A.; Douglas, J. *J. Catal.* **1985**, *96*, 535–543.
(32) Chantal, P. D.; Kaliaguine, S.; Grandmaison, J. L. *Appl. Catal.* **1985**, *18*, 133–145.
(33) Kallury, R. K. M.; Tidwell, T. T.; Boocock, D. G. B.; Chow, D. H. L. *Can. J. Chem.* **1984**, *62*, 2540–2545.
(34) Adjaye, J. D.; Bakhshi, N. N. *Biomass Bioenergy* **1995**, *8*, 131–149.
(35) Zhu, X.; Mallinson, R. G.; Resasco, D. E. *Appl. Catal., A: Gen.* **2010**, *379*, 172–181.
(36) Girgis, M. J.; Gates, B. C. *Ind. Eng. Chem. Res.* **1991**, *30*, 2021–2058.
(37) Bredenberg, J. B.; Huuska, M.; Räty, J.; Korpio, M. *J. Catal.* **1982**, *77*, 242–247.
(38) Hurff, S. J.; Klein, M. T. *Ind. Eng. Chem. Res.* **1983**, *22*, 426–430.
(39) Runnebaum, R. C.; Nimmanwudipong, T.; Block, D. E.; Gates, B. C. *Catal. Lett.* **2011**, *141*, 817–820.
(40) Nimmanwudipong, T.; Runnebaum, R. C.; Block, D. E.; Gates, B. C. *Catal. Lett.* **2011**, *141*, 779–783.
(41) Nimmanwudipong, T.; Runnebaum, R. C.; Tay, K.; Block, D. E.; Gates, B. C. *Catal. Lett.* **2011**, *141*, 1072–1078.
(42) Nimmanwudipong, T.; Runnebaum, R. C.; Block, D. E.; Gates, B. C. *Energy Fuels* **2011**, *25*, 3417–3427.
(43) Bhore, N. A.; Klein, M. T.; Bischoff, K. B. *Ind. Eng. Chem. Res.* **1990**, *29*, 313–316.
(44) Bhore, N. A.; Klein, M. T.; Bischoff, K. B. *Chem. Eng. Sci.* **1990**, *45*, 2109–2116.
(45) Zhao, C.; Kou., Y.; Lemonidou, A. A.; Li, X.; Lercher, J. A. *Angew. Chem., Int. Ed.* **2009**, *48*, 1–5.
(46) Şenol, O. İ.; Ryymin, E. −M.; Viljava, T. −R.; Krause, A. O. I. *J Mol. Catal. A: Chem.* **2007**, *277*, 107–112.
(47) Gutierrez, A.; Kaila, R. K.; Honkela, M. L.; Slioor, R.; Krause, A. O. I. *Catal. Today* **2009**, *147*, 239–246.